

# Influence of Compatibilizers on Mechanical Properties, Crystallization, and Morphology of Polypropylene/Scrap Rubber Dust Blends

P. Phinyocheep,<sup>1,2</sup> F. H. Axtell,<sup>3</sup> T. Laosee<sup>1</sup>

<sup>1</sup> Department of Chemistry, Faculty of Science, Mahidol University, Rama VI Road, Payathai, Bangkok 10400, Thailand

<sup>2</sup> The Polymer Technology Research and Development Center, Institute of Science and Technology for Research and Development, Salaya Campus, Nakorn Pathom 73170, Thailand

<sup>3</sup> Dry Color Pacific Limited, 31 Rama III Road, Yanawa, Bangkok 10120, Thailand

Received 30 October 2001; accepted 10 January 2002

**ABSTRACT:** Polypropylene blends containing a dispersed phase of scrap rubber dusts obtained from sport shoes manufacture; midsole (M, vulcanized EVA foam) and outsole (O, vulcanized rubber blend of NR, SBR, and BR) were studied. The influence of various compatibilizers on the mechanical properties of these blends were investigated. Significant development of impact strength was attained by using 6 and 10 phr of styrene–ethylene–butylene–styrene (SEBS) and maleic anhydride-grafted styrene–ethylene–butylene–styrene (SEBS-g-MA) as compatibilizers for both compounds filled with midsole and outsole dusts. The tensile strength of each compound was slightly decreased when the compatibilizer loading increased, whereas the elongation at break was significantly increased. The enhancements of the impact strength and

the elongation at break are believed to arise from reduction of interfacial tension between two phases of the rubber and the PP, which results in some reduction of the particle size of the fillers. Scanning electron microscopy (SEM) confirmed the evidence of the reduction of scrap rubber dust into small rubber particle sizes in the compound, and also showed the occurrence of some fibrils. Optical microscopy (crossed polars) observations suggested that the addition of the rubber dust resulted in a less regular spherulite texture and less sharp spherulite boundaries. © 2002 Wiley Periodicals, Inc. *J Appl Polym Sci* 86: 148–159, 2002

**Key words:** mechanical properties; crystallization; blends; compatibilization; recycling

## INTRODUCTION

Blending of two different polymers is an effective and economically viable way for production of new materials with desired properties. This technique has expanded rapidly into the rubber toughening of both thermoplastic and thermoset systems for achieving properties suited to particular applications.<sup>1</sup> In addition, potential uses of waste materials are developed by this technology.<sup>2–5</sup> However, performance of such two-phase polymer blends depends mainly on its degree of compatibility and morphology developed during the processing. A large number of works dealing with isotactic polypropylene (PP)-based blends has been continuously reported throughout the past two decades. For the production of high-impact PP, various elastomers have been investigated as impact modifiers. The studies of rubber modification of polypropylene are mostly confined to using ethylene propylene rubber (EPR),<sup>6–11</sup> ethylene–propylene–diene

terpolymer (EPDM),<sup>12–17</sup> and styrene–ethylene–butylene–styrene copolymer (SEBS).<sup>18–20</sup> Some other elastomeric materials that can also be used as a toughening agent for PP are ethylene vinyl acetate (EVA), polybutadiene, and natural rubber.<sup>21–24</sup> Blending of PP with cryogenically ground rubber and vulcanized rubber dust<sup>2–5,25,26</sup> were interestingly investigated for the point of disposal of waste and the reduction in product cost. It has been found in most of the works that the important factors in rubber toughening of PP include (1) rubber content, (2) rubber particle size and particle size distribution, (3) degree of crosslinking, (4) degree of interfacial adhesion, and (5) spherulite size and spherulite boundary of PP.

It is known that the rubber modifier particles in the matrix act as stress concentrators of the applied stress. Various deformation mechanisms have been proposed to explain the toughening of polymers with elastomeric particles. These include stress relief by cavitation around rubber particles, matrix crazing, shear yielding, and combined crazing and yielding.<sup>27</sup> Generally the optimum rubber particle size in the case of pseudoductile polymer is about 0.1–0.5  $\mu\text{m}$ .<sup>5,13</sup> By contrast, for a brittle polymer such as polystyrene it is 1–3  $\mu\text{m}$ . Clearly, scrap rubbers, even when ground to the smallest size possible, are still an order of magni-

Correspondence to: P. Phinyocheep (scppo@mahidol.ac.th).

Contract grant sponsor: National Metal and Materials Technology Center.

**TABLE I**  
**Types and Characteristic of Compatibilizers**

Compatibilizer	Supplier	Composition by weight	Copolymer $\bar{M}_n \times 10^{-3}$	End block $\bar{M}_n \times 10^{-3}$	Mid block $\bar{M}_n \times 10^{-3}$
1. SBS (Cariflex TR 1102)	Shell Chemical Co. Ltd.	28% styrene	88.0	8.8	70.4
2. SEBS (Kraton G 1652)	Shell Chemical Co. Ltd.	29% styrene	51.5	7.0	37.5
3. SEBS-g-MA (Kraton FG-1901X)	Shell Chemical Co. Ltd.	29% styrene, 1.84% MA	NA	NA	NA
4. PE-g-MA	Mitsui Co. Ltd.	0.36% MA <sup>a</sup>	NA	NA	NA
5. PP-g-MA	<sup>b</sup>	0.6% MA	87	NA	NA
6. PP-g-GMA	<sup>b</sup>	0.6% MA	87	NA	NA

<sup>a</sup> Elemental analysis, NA: not available.

<sup>b</sup> Supplied by Professor Guo-Hua Hu, Laboratoire des Sciences du Génie Chimique, Ecole Européenne d'Ingénieurs en Génie des Matériaux, CNS-ENSIC-INPL, 1, rue Grandville, B.P. 451, 54001 Nancy Cedex, France.

tude larger than the optimum size. The rubber, therefore, when incorporation in a thermoplastic matrix is most likely acting as a filler. Emphasis is, therefore, given to the adhesion between the scrap rubber dust and the matrix polymer for the improvement of mechanical properties of such composites. The need for an interfacial adhesion promoter came into account. Generally, addition of a third component or a compatibilizer into a binary blend should render a blend compatibility whereby the resultant blend displays homogeneous and fine morphology of the minor phase in the matrix polymer.<sup>28-35</sup> The compatibilizers act as a polymeric surfactant, lowering surface tension and promoting interfacial adhesion between different phases in a polymer blend. They can also influence in the reduction of the physical size of the domains, and stabilize the morphology of the blends.

In this study, great attention has been paid to the reuse of waste rubbers obtained from sport shoe manufacture as toughening additives for polypropylene. The waste rubbers are vulcanized rubbers generated in the form of rubber dusts in the buffing stage of the sole components (midsole, which is a vulcanized EVA foam, and outsole, which is a vulcanized rubber blend of NR, BR, and SBR). As is well known, the dissimilarity in their structures of the PP and these rubber dusts, the polymer blend is incompatible. Therefore, no considerable improvement in impact strength was found in our previous works.<sup>25,26</sup> Addition of a compatibilizer to the blend system to improve interfacial adhesion between the phases was our major interest.

In this article we report the effect of six different types of compatibilizers, i.e., styrene-butadiene-styrene (SBS), styrene-ethylene-butylene-styrene (SEBS), maleic anhydride-grafted styrene-ethylene-butylene-styrene (SEBS-g-MA), maleic anhydride-grafted polyethylene (PE-g-MA), maleic anhydride-grafted polypropylene (PP-g-MA), and glycidyl methacrylate-grafted polypropylene (PP-g-GMA) as well as compatibilizer loading on the mechanical properties of polypropylene/scrap rubber dust compounds. The thermal properties, morphology, and crystallization of the blends influenced by the compatibilizers were also investigated.

## EXPERIMENTAL

### Materials and compound formulations

Isotactic polypropylene (PP) injection grade 6331 was obtained from HMC Co. Ltd., Thailand (melt flow index 12.0 g per 10 min). Two types of scrap rubber dusts were obtained from buffing process in sport shoe soles manufacture, midsole (M, vulcanized EVA foam), and outsole (O, vulcanized rubber blend of NR, BR, and SBR) supplied by Piyavat Rubber Industry Co. Ltd., Thailand. Various types of compatibilizers used in this study are shown in Table I. Ultrinox 626, used as an antioxidant, is the product from GE Speciality Chemicals, supplied by Nagase (Thailand) Co. Ltd.. The compound formulation of polypropylene and scrap rubber dusts is shown in Table II.

**TABLE II**  
**Compound Formulation of Polypropylene/Scrap Rubber Dusts**

Material	M(0)	M(2)	M(6)	M(10)	O(0)	O(2)	O(6)	O(10)
PP (% by weight)	75	75	75	75	75	75	75	75
Midsole (% by weight)	25	25	25	25	—	—	—	—
Outsole (% by weight)	—	—	—	—	25	25	25	25
Compatibilizer (phr)	—	2	6	10	0	2	6	10
Ultrinox 626 (phr)	1	1	1	1	1	1	1	1
Total	101	103	107	111	101	103	107	111

**TABLE III**  
Charpy Notched Impact Strength, I.S. ( $\text{kJ}/\text{m}^2$ ), Rubber Particle Size, and Particle Size Distribution of PP/Scrap Rubber Dust (75:25) Compound

Compound	Average I.S. ( $\text{kJ}/\text{m}^2$ )	Mean diameter ( $\mu\text{m}$ )	Range ( $\mu\text{m}$ )
PP	4.0	—	—
PP/midsole	4.1	8.6	1.2–190.5
PP/outsole	4.4	8.7	1.2–170.0

### Masterbatch preparation

Masterbatch containing polypropylene, scrap rubber dust, and compatibilizer of composition 30 : 50 : 20 by weight, respectively, were prepared with an Internal mixer (Chang Tong 1655). All of the ingredients were mixed by tumble mixer to give a random distribution before compounding in the mixer. The mixer speed was 70 rpm, and mixing time was 20 min. The mixed materials were sheeted on a two-roll mill before granulation with a granulator.

### Compounding

Polypropylene, scrap rubber dust, masterbatch, and antioxidant with formulation shown in Table II were mixed by a tumble mixer to give a random distribution before compounding in a single screw extruder [Betol 3225] (screw diameter 32 mm), UK; L/D = 25 : 1] connected with a SD-CTM [self-driven cavity transfer mixer, Iddon (screw diameter 30 mm), UK]. The temperature profile of the single screw was 190/200/210/220/220 $^{\circ}\text{C}$ , and the temperature profile of the SD-CTM was 220/220 $^{\circ}\text{C}$ . The screw speed of the single screw extruder and SD-CTM were 35 and 60 rpm, respectively. The extrudate was cooled in a water bath, and it was later granulated with a granulator into granule form ready for injection molding into testing specimens of impact and tensile bars.

### Mechanical properties testing

Charpy impact strength testing of the notched specimens according to ASTM A-2436 was conducted using an impact tester (Zwick) with 2.7 Joule pendulum. Tensile properties of the dumbbell-shape specimen were measured according to ISO 527 type B, using an Instron mechanical tester (model 4301), with grip length of 50 mm, crosshead speed of 50 mm  $\text{min}^{-1}$ , and a full scale load of 100 kg. The average value and standard deviation of the impact and tensile properties were calculated using at least 20 samples.

### Particle size and particle size distribution

A thin section of 3–5  $\mu\text{m}$  thickness of the PP compound was produced by using microtome apparatus

(Polycut). It was then placed under a 10 $\times$  objective lens of an optical microscope connected to an image analyzer (Omminet 4, Buchler, USA.) to evaluate the particle size and particle size distribution of the rubber dusts.

### Thermal measurements

The PP crystallization behavior was analyzed by using differential scanning calorimeter, DSC (Perkin-Elmer DSC-7) under nitrogen atmosphere. About 10 mg of the samples was cut from the impact bars at the core position. The scanning temperature was raised from 70 to 240 $^{\circ}\text{C}$  at a rate of 10 $^{\circ}\text{C}/\text{min}$  and then held at 240 $^{\circ}\text{C}$  for 3 min to erase the thermal history, and it was swept back to 70 $^{\circ}\text{C}$  at 10 $^{\circ}\text{C}/\text{min}$ .

### Crystallization texture

The crystallite texture of PP was evaluated by polarizing microscope (Olympus). A thin section of 3–5  $\mu\text{m}$  thickness produced by using microtome apparatus (Polycut) was analyzed by using a 40 $\times$  objective lens.

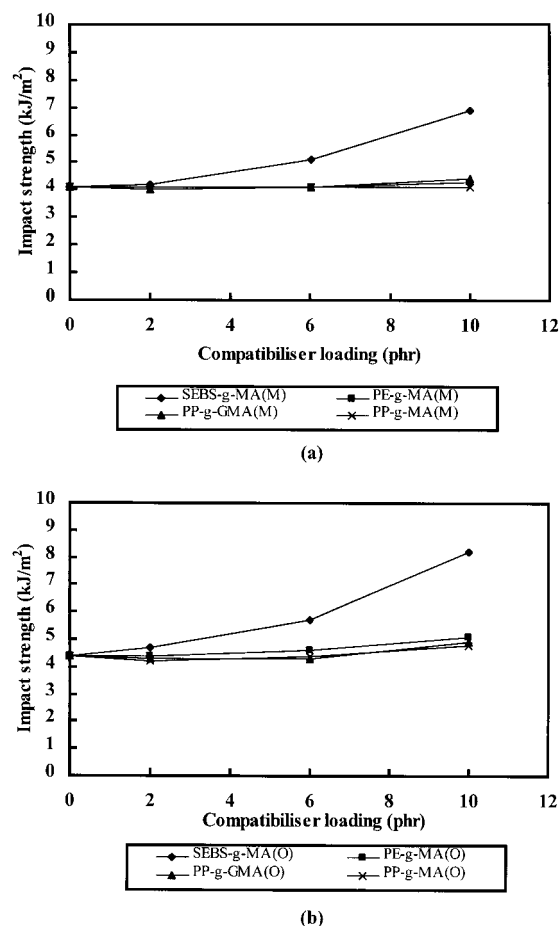


**Figure 1** Effect of polar compatibilizer type and compatibilizer loading on Charpy notched impact strength ( $\text{kJ}/\text{m}^2$ ) of (a) PP/midsole compounds, (b) PP/outsole compounds.

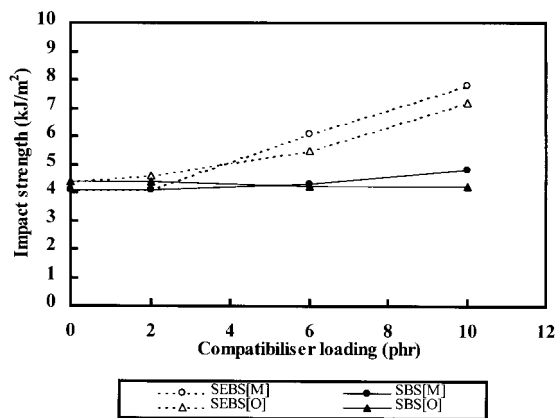


Figure 2 Effect of nonpolar compatibilizer type and compatibilizer loading on Charpy notched impact strength (kJ/m<sup>2</sup>) of PP/scrap dust compounds.

**Morphology**

Scanning electron microscope (SEM, Hitachi S-2500) at 15 kV accelerated voltage was used to explore the morphology of the PP compound. Three types of specimens used were the broken part of the impact bar after testing. The first one was used directly, while the second and the third type were immersed in liquid nitrogen for 2 h before fracture and then etched with xylene for 24 h, respectively. The samples were mounted on SEM stubs then sputter coated with palladium.

**RESULTS AND DISCUSSION**

**Mechanical properties of the PP compounds**

**Impact strength**

The impact property of a thermoplastic is often increased by the addition of a rubber phase, i.e., the

rubber phase helps in toughening the matrix polymer. For incorporation of particulate scrap rubber into polymer matrix, the particle size of the rubber and the adhesion between the polymer matrix and ground rubber are believed to be major factors controlling the mechanical properties of the composites.<sup>2,7,12,13</sup> Table III shows that addition of scrap rubber dust to polypropylene (PP) matrix did not result in improving but rather maintaining the impact properties of PP. This may be due to insufficient adhesion between the two phases; the rubber particle cannot play a role of energy transfer in the composite. If no adhesion exists, voiding will occur at the interface and major crack propagation is likely in both tensile and impact testing. In addition, the rubber particle size of midsole and outsole dust, which are 8.6 and 8.7 μm, respectively, are an order of magnitude larger than the optimum size of rubber toughening agents normally employed for pseudoductile polymer.<sup>5,13</sup> Therefore, an interfacial adhesion promoter for the scrap rubber dust and the PP matrix phases was considered for the improvement of mechanical properties of such composites. Using a compatibilizer, which may alter the adhesion between the two dissimilar phases and most probably stabilize the distribution of rubber in the matrix, can increase the interfacial adhesion. In this study, two groups of compatibilizers, polar and nonpolar materials, were employed. The polar compatibilizers considered are SEBS-g-MA, PE-g-MA, PP-g-GMA, and PP-g-MA, while the nonpolar ones are SBS and SEBS.

Figure 1 shows that in the case of polar compatibilizers used for PP/scrap rubber dust compounds, the functional polymer as SEBS-g-MA gave the best impact strength of PP/scrap rubber dust compounds both for midsole and outsole, particularly when 10 phr of SEBS-g-MA were used. For nonpolar compatibiliz-

TABLE IV  
Effect of Polar Compatibilizer Type and Loading on Charpy Notched Impact Strength, I.S. (kJ/m<sup>2</sup>), Rubber Particle Size, and Particle Size Distribution of PP/Scrap Dust Compounds

Polar compatibilizer				PP/midsole compound			PP/outsole compound		
SEBS-g-MA (phr)	PE-g-MA (phr)	PP-g-GMA (phr)	PP-g-MA (phr)	Average I.S. (kJ/m <sup>2</sup> )	Mean diameter (μm)	Range (μm)	Average I.S. (kJ/m <sup>2</sup> )	Mean diameter (μm)	Range (μm)
0				4.1	8.6	1.2-190.5	4.4	8.7	1.2-170.0
2				4.2	6.8	1.2-185.5	4.7	7.0	1.2-172.9
6				5.1	6.1	1.2-115.9	5.7	5.7	1.2-172.4
10				6.9	5.7	1.2-83.1	8.2	5.4	1.2-106.8
	2			4.1	6.6	1.2-164.0	4.4	6.8	1.2-187.5
	6			4.1	6.5	1.2-163.6	4.6	6.5	1.2-120.1
	10			4.3	5.5	1.2-150.0	5.1	5.7	1.2-127.1
		2		4.0	6.9	1.2-120.8	4.3	7.3	1.2-107.5
		6		4.1	7.0	1.2-126.7	4.3	6.4	1.2-111.9
		10		4.4	7.0	1.2-138.9	4.9	6.4	1.2-99.7
			2	4.0	7.4	1.2-131.4	4.2	6.5	1.2-193.8
			6	4.1	6.6	1.2-88.5	4.4	6.4	1.2-130.6
			10	4.1	6.6	1.2-104.4	4.8	6.0	1.2-122.5

TABLE V  
Effect of Nonpolar Compatibilizer on Charpy Notched Impact Strength, I.S. (kJ/m<sup>2</sup>), Particle Size, and Particle Size Distribution of PP/Scrap Dust Compounds

Nonpolar compatibilizer		PP/midsole compound			PP/outsole compound		
SEBS (phr)	SBS (phr)	Average I.S. (kJ/m <sup>2</sup> )	Mean diameter (μm)	Range (μm)	Average I.S. (kJ/m <sup>2</sup> )	Mean diameter (μm)	Range (μm)
0		4.1	8.6	1.2–190.5	4.4	8.7	1.2–170.0
2		4.1	6.5	1.2–122.7	4.6	6.9	1.2–117.3
6		6.1	5.7	1.2–137.3	5.5	6.5	1.2–121.5
10		7.8	5.5	1.2–94.5	7.2	5.9	1.2–118.3
	2	4.1	7.0	1.2–130.6	4.4	7.5	1.2–120.4
	6	4.3	6.7	1.2–93.1	4.2	6.6	1.2–111.7
	10	4.8	5.7	1.2–84.2	4.2	6.2	1.2–184.6

ers, SBS and SEBS, which have been used as impact modifiers in thermoplastics,<sup>11,19,20,33</sup> show their effect in Figure 2. The compounds of both midsole and outsole compatibilized with SEBS gave better Charpy notched impact strength than the use of SBS. The results in Table IV indicate that the Charpy notched impact strength increased approximately 70% for PP/midsole/SEBS-g-MA compound and 86% for PP/outsole/SEBS-g-MA compounds, whereas PE-g-MA, PP-g-GMA, and PP-g-MA resulted in nearly unchanged Charpy notched impact strength of both compatibilized PP/midsole and PP/outsole compounds. For PP/midsole/SEBS compound and PP/outsole/SEBS compounds the Charpy notched impact strength increased approximately by 90 and 63%, respectively (Table V). The higher impact strength of the compound compatibilized with SEBS or SEBS-g-MA than the compound compatibilized with SBS can be ex-

plained that the EB midblock of the SEBS copolymer gave better compatibility with PP than the B (butadiene) midblock of the SBS copolymer. This explanation is in accordance with the work of Setz et al.<sup>19</sup> It had been shown that PP has good compatibility with the EB block copolymer because of the repulsion effect of ethene and but-1-ene segments that might contribute to the improvement of the miscibility of PP with scrap rubber dust.

Tables IV and V show also that addition of compatibilizers both polar and nonpolar types into PP/M and PP/O gave smaller particle size than in uncompatibilized compound. It was found that PP/rubber dust compounds compatibilized with 10 phr SEBS and SEBS-g-MA both midsole and outsole gave smaller rubber particle size than other types and loading of the compatibilizer. The mean diameter and range of dust particle size in the PP/M/10 phr SEBS-g-MA

TABLE VI  
Tensile Yield Strength, Modulus, and Elongation at Break of the Compatibilized PP/Midsole Compounds

Code	Yield strength (MPa)		Modulus (MPa)		Elongation at break (%)	
	Average	SD	Average	SD	Average	SD
PP	33.8	2.2	942.0	30.1	581	36.7
PP/M	23.3	0.2	651.3	21.6	19	2.9
PP/M/SBS(2)	23.0	0.2	650.6	27.8	23	5.4
PP/M/SBS(6)	22.6	0.2	635.8	18.1	29	5.3
PP/M/SBS(10)	22.0	0.2	609.3	15.2	48	7.8
PP/M/SEBS(2)	23.5	0.3	683.2	13.9	35	5.6
PP/M/SEBS(6)	22.3	0.3	655.1	7.7	177	44.8
PP/M/SEBS(10)	21.9	0.2	599.9	28.2	458	43.6
PP/M/SEBS-g-MA(2)	23.2	0.4	645.9	16.8	25	5.0
PP/M/SEBS-g-MA(6)	23.2	0.3	618.7	12.4	91	34.9
PP/M/SEBS-g-MA(10)	22.3	0.2	587.0	16.0	411	77.6
PP/M/PE-g-MA(2)	23.6	0.2	649.0	17.1	18	2.6
PP/M/PE-g-MA(6)	23.8	0.2	649.6	12.4	24	2.9
PP/M/PE-g-MA(10)	23.1	0.2	627.8	13.4	41	9.2
PP/M/PP-g-MA(2)	25.0	0.3	699.8	15.9	23	5.0
PP/M/PP-g-MA(6)	25.4	0.4	701.3	22.8	23	3.6
PP/M/PP-g-MA(10)	26.4	0.2	730.6	24.0	31	8.1
PP/M/PP-g-GMA(2)	24.7	0.3	689.2	23.9	21	4.0
PP/M/PP-g-GMA(6)	25.1	0.4	707.0	31.9	23	5.6
PP/M/PP-g-GMA(10)	26.1	0.3	730.8	31.6	37	5.9



**TABLE VII**  
**Tensile Yield Strength, Modulus, and Elongation at Break of the Compatibilized PP/Outsole Compounds**

Code	Yield strength (MPa)		Modulus (MPa)		Elongation at break (%)	
	Average	SD	Average	SD	Average	SD
PP	33.8	2.2	942.0	30.1	581	36.7
PP/O	20.0	0.7	575.4	21.1	10	3.0
PP/O/SBS(2)	19.8	0.4	589.7	13.1	10	2.4
PP/O/SBS(6)	20.6	0.7	584.0	29.7	23	4.3
PP/O/SBS(10)	19.4	0.6	559.2	20.0	33	4.8
PP/O/SEBS(2)	20.3	0.5	615.1	22.1	14	4.0
PP/O/SEBS(6)	20.8	0.3	619.8	20.4	23	1.0
PP/O/SEBS(10)	20.5	0.2	592.0	13.1	52	26.7
PP/O/SEBS-g-MA(2)	20.0	0.4	574.9	15.4	15	3.7
PP/O/SEBS-g-MA(6)	20.5	0.3	576.0	21.5	30	6.2
PP/O/SEBS-g-MA(10)	19.9	0.2	551.0	17.1	62	14.3
PP/O/PE-g-MA(2)	20.4	0.5	583.0	21.8	11	1.7
PP/O/PE-g-MA(6)	21.5	0.3	601.1	22.5	19	3.3
PP/O/PE-g-MA(10)	21.5	0.2	583.8	16.2	34	6.8
PP/O/PP-g-MA(2)	22.4	0.5	653.4	29.0	10	2.0
PP/O/PP-g-MA(6)	23.3	0.3	650.6	19.1	20	5.6
PP/O/PP-g-MA(10)	23.8	0.3	665.4	20.0	35	6.7
PP/O/PP-g-GMA(2)	21.9	0.6	632.1	21.8	10	3.2
PP/O/PP-g-GMA(6)	23.5	0.4	654.3	19.9	27	5.2
PP/O/PP-g-GMA(10)	24.3	0.3	672.1	23.3	47	15.6

compound were 5.7 and 1.2–83.1  $\mu\text{m}$ , respectively. A Charpy notched impact strength of 6.9  $\text{kJ}/\text{m}^2$  was obtained. In contrast, the mean diameter and range of dust particle size in the PP/M/10 phr PP-g-MA compound were 6.6 and 1.2–104.4  $\mu\text{m}$ , respectively. The compound had a low impact strength (4.1  $\text{kJ}/\text{m}^2$ ). In the case of PP/O/10 phr SEBS-g-MA compound, the mean diameter and range of particle size of the dust were 5.4 and 1.2–106.8  $\mu\text{m}$ , respectively, whereas the mean diameter and range of dust particle size in PP/outsole/10 phr PP-g-MA were 6.0 and 1.2–122.5  $\mu\text{m}$ , respectively. This is corresponding with the value of impact strength in the PP/O/SEBS-g-MA (8.2  $\text{kJ}/\text{m}^2$ ) and PP/O/PP-g-MA (4.8  $\text{kJ}/\text{m}^2$ ). It can also be seen that in PP/outsole compatibilized by SEBS-g-MA gave lower dust particle size than in PP/midsole compatibilized by SEBS-g-MA, and it gave higher impact strength. Therefore, the decrease in the rubber particle size was responsible for the increase of impact strength as has ever been reported.<sup>11–13</sup> Comparing between the rubber particle size and impact properties of PP compounds, it can be concluded that a good compatibilizer helps in stabilization of the rubber particle resulted in smaller particle size of the dust, and hence, a higher impact property.

**Tensile properties**

The tensile properties of PP, 75/25 PP/scrap rubber dust compounds with and without various types and loading of compatibilizers were investigated, and the results are shown in Tables VI and VII. When PP was modified by adding 25% scrap rubber dust, the tensile

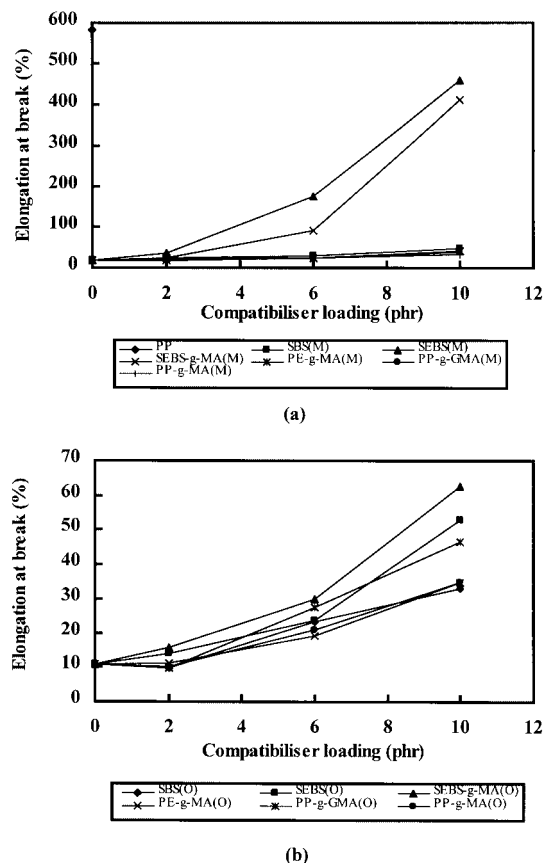


**Figure 3** Elongation at break of the compatibilized compounds; (a) PP/midsole compound, (b) PP/outsole compound.

TABLE VIII  
Thermal Analysis of Compatibilized PP/Midsole Compound from the Cooling Curve of DSC

Code	Range temp.	$T_p$	$T_{onset}$	$S_i$	$\Delta W$	$\Delta H_{pp}$
PP	92.3–126.3	108.2	114.3	84.0	5.9	91.57
PP/M	101.9–127.9	116.7	121.4	86.0	5.4	100.61
PP/M/SBS(2)	101.3–124.7	113.9	118.1	86.5	4.5	98.31
PP/M/SBS(6)	98.7–123.7	113.0	117.0	87.0	4.3	99.29
PP/M/SBS(10)	97.1–121.8	112.5	116.7	87.0	4.3	99.91
PP/M/SEBS(2)	97.9–125.7	114.5	118.7	86.5	4.3	99.50
PP/M/SEBS(6)	93.9–121.8	111.9	115.8	88.0	3.9	102.61
PP/M/SEBS(10)	98.7–123.7	113.0	116.9	87.5	3.8	99.37
PP/M/SEBS-g-MA(2)	98.7–124.7	116.1	120.2	88.0	4.4	99.10
PP/M/SEBS-g-MA(6)	98.7–122.6	112.4	116.6	87.0	4.3	97.59
PP/M/SEBS-g-MA(10)	100.3–124.7	112.5	116.7	86.0	4.3	97.69
PP/M/PE-g-MA(2)	102.4–125.8	116.7	120.9	87.0	4.9	98.67
PP/M/PE-g-MA(6)	101.9–122.6	113.0	116.9	85.0	3.9	97.45
PP/M/PE-g-MA(10)	101.9–123.9	112.5	116.2	84.0	3.7	96.61
PP/M/PP-g-GMA(2)	101.9–128.2	117.4	121.6	87.5	4.3	103.00
PP/M/PP-g-GMA(6)	105.1–129.5	118.1	121.7	86.0	3.8	107.59
PP/M/PP-g-GMA(10)	101.9–128.9	117.2	121.1	87.0	4.1	110.62
PP/M/PP-g-MA(2)	105.1–130.6	119.3	123.2	87.0	4.1	99.03
PP/M/PP-g-MA(6)	105.1–132.2	120.8	124.8	86.5	4.0	105.82
PP/M/PP-g-MA(10)	106.7–132.2	121.6	125.6	87.0	3.9	109.74

yield strength, modulus, and elongation at break were decreased because of the incompatibility of the phases in the compound.<sup>8,14,16</sup> In the incompatible compounds, the adhesion between the phases was poor, and then microvoids at interface occurred, resulting in deterioration of mechanical properties of the compounds. When the compounds were compatibilized with SBS, SEBS, SEBS-g-MA, and PE-g-MA, the tensile yield strength and modulus of the compounds were decreased. This effect is more pronounced when higher amount of compatibilizers was used. This can be explained by the plasticising effect of PP. However,

in the case of compound compatibilized by PP-g-MA and PP-g-GMA, a slight increase of the tensile yield strength and modulus of the compounds were observed. This may come from the fact that the tensile strength of the PP-g-MA and PP-g-GMA is higher than SBS, SEBS, SEBS-g-MA, and PE-g-MA. It was also found from thermal analysis that the degree of crystallinity of the PP phase in the PP compound compatibilized by PP-g-MA and PP-g-GMA was higher than in the compound compatibilized by SBS, SEBS, SEBS-g-MA, and PE-g-MA.

Generally, the elongation at break of rubber filled

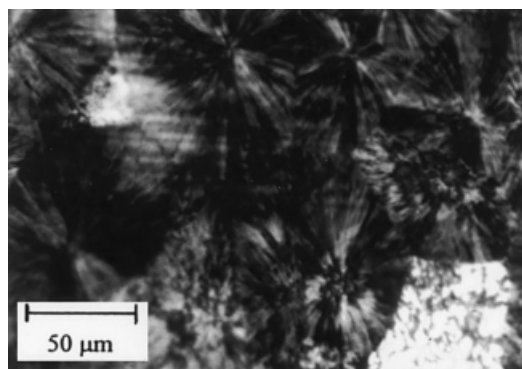
TABLE IX  
Thermal Analysis of Compatibilized PP/Outsole Compound from the Cooling Curve of DSC

Code	Range temp.	$T_p$	$T_{onset}$	$S_i$	$\Delta W$	$\Delta H_{pp}$
PP	92.3–126.3	108.2	114.3	84.0	5.9	91.57
PP/O	101.3–126.0	116.1	120.6	86.0	4.5	96.72
PP/O/SBS(2)	102.1–126.6	115.1	119.7	86.0	4.6	101.62
PP/O/SBS(6)	101.9–123.1	113.4	117.7	84.0	4.4	99.13
PP/O/SBS(10)	100.3–123.4	114.1	118.2	86.0	4.4	98.77
PP/O/SEBS(2)	89.1–127.4	116.2	121.0	89.0	4.6	107.56
PP/O/SEBS(6)	95.5–126.8	115.9	120.8	89.0	4.9	100.78
PP/O/SEBS(10)	92.3–127.4	115.8	120.7	88.0	4.9	106.36
PP/O/SEBS-g-MA(2)	82.8–125.5	115.2	120.2	91.0	4.8	102.95
PP/O/SEBS-g-MA(6)	89.1–125.0	114.8	119.5	91.0	4.8	97.89
PP/O/SEBS-g-MA(10)	89.1–124.5	114.6	119.0	91.0	4.4	99.23
PP/O/PE-g-MA(2)	96.0–127.4	116.4	120.8	86.5	4.5	101.73
PP/O/PE-g-MA(6)	95.5–126.6	115.5	119.9	85.5	4.5	99.99
PP/O/PE-g-MA(10)	102.4–125.0	115.1	118.9	81.0	4.0	97.68
PP/O/PP-g-GMA(2)	105.1–129.8	118.8	122.6	86.0	4.0	105.60
PP/O/PP-g-GMA(6)	105.1–131.4	119.8	123.6	87.0	4.0	107.79
PP/O/PP-g-GMA(10)	105.9–131.4	120.4	124.3	86.0	3.9	110.84
PP/O/PP-g-MA(2)	101.9–132.2	119.7	123.6	86.0	3.9	106.59
PP/O/PP-g-MA(6)	103.5–131.4	120.4	124.3	87.0	3.9	106.79
PP/O/PP-g-MA(10)	106.92–131.35	120.9	124.9	85.0	4.0	109.12

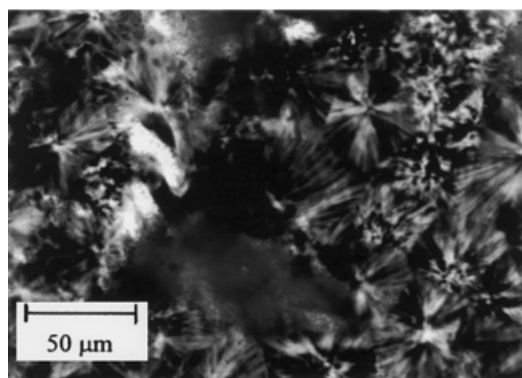
thermoplastic increases if there is sufficient adhesion between the matrix and the rubber. It can be seen in Figure 3 that an increase in elongation at break was achieved for all the compatibilized compounds compared to the uncompatibilized compounds. Particularly, for PP/midsole compounds compatibilized with 10 phr SEBS and 10 phr SEBS-*g*-MA, the best elongation at break was significantly increased up to 458% for SEBS and 411% for SEBS-*g*-MA. This is due to sufficient adhesion between the matrix phase and the dispersed phase; hence, efficient stress transfer from the matrix to the dispersed phase occurred, resulting in an increase of elongation at break. However, for PP/outsole compounds compatibilized with 10 phr SEBS and 10 phr SEBS-*g*-MA, the best elongation at break was increased only up to 52% for SEBS and 62% for SEBS-*g*-MA. This is thought to be because the midsole dust had better compatibility with PP than the outsole dust when SEBS was used, and hence, slower crack growth due to dissipating energy in the plastic deformation region.

### Crystallization behavior

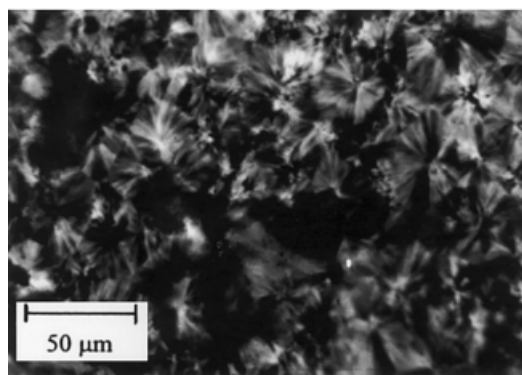
It has been reported that elastomers added to the PP compound act as nucleating agents, and cause significant modification in the morphology and thermal behavior of the PP.<sup>10,14,18,23,36,37</sup> The crystallization behavior of PP in PP compounds was investigated by differential scanning calorimeter (DSC) to detect the change in melting and the degree of crystallization. Generally, the presence of an elastomer can affect the crystallization exotherm, which can be characterized by determining (1) the exothermic peak temperature ( $T_p$ ) determined as the point of intersection of the tangents by the two sides of the exotherm, (2) the onset temperature ( $T_{onset}$ ) determined as the point of intersection of the baseline and the tangent of the high temperature side of the exotherm, (3) the slope of initial portion of exotherm ( $S_i$ ), (4) the width at half-height of the exotherm peak ( $\Delta W$ ), and (5) the area under the peak per unit weight of the crystallizable component of the sample ( $\Delta H_{PP}$ ). The nonisothermal crystallization data from the cooling curve of DSC analysis of the neat PP, PP/midsole, PP/outsole, and compatibilized PP/scrap dust compounds are shown in Tables VIII and IX. In the presence of midsole and outsole, the crystallization peak of the PP ( $T_p$ ) is shifted towards a higher temperature. The neat PP crystallizes between 92.3 and 126.3°C, and the temperature position of  $T_p$  is at 108.2°C. When PP crystallizes in the presence of midsole and outsole, the crystallization peaks shift to 116.7 and 116.1°C, with a temperature range of 101.9–127.9 and 101.3–126.0°C, respectively. Such finding indicates that the scrap rubber dusts both midsole and outsole possesses nucleating ability on the crystallization process of the PP; the



(a)



(b)



(c)

**Figure 4** Optical micrographs of unfilled PP and filled PP, crossed polars; (a) neat PP, (b) PP/midsole, (c) PP/outsole.

observation of heterogeneous nucleation of PP from the surface of the scrap rubber dust particles (see Fig. 4).

For the compatibilized compounds, compatibilization with SBS, SEBS, SEBS-*g*-MA, and PE-*g*-MA caused a decrease in peak temperature ( $T_p$ ), which continued to decline slowly with increasing compatibilizer loading in both the PP/midsole and PP/outsole compound. The SBS, SEBS, SEBS-*g*-MA, and PE-*g*-MA acting as a retarding agent in the compounds may have caused this, whereas the composition con-



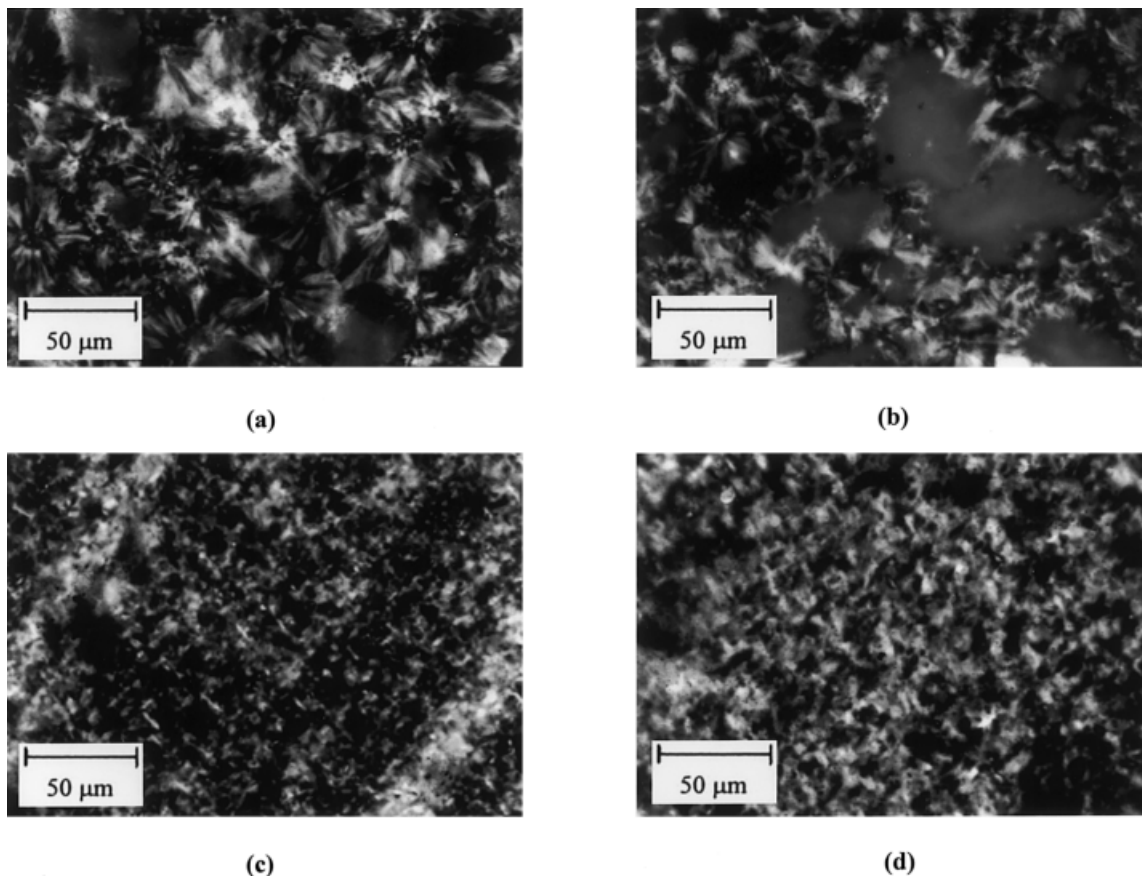


**Figure 5** Optical micrographs of PP/scrap dust compound compatibilized with SEBS and PP-g-MA, crossed polars; (a) PP/M/10 phr SEBS, (b) PP/O/10 phr SEBS, (c) PP/M/10 phr PP-g-MA, (d) PP/O/10 phr PP-g-MA.

taining PP-g-MA and PP-g-GMA as compatibilizers exhibited a slight increase in peak temperature, which continued to increase slowly with increased compatibilizer loading. This may have been caused by the PP-g-MA and PP-g-GMA acting as nucleating agents in the compounds.

It was found that  $S_i$  of the compatibilized PP blend is higher than the pure PP, whereas  $\Delta W$  is lower than the pure PP. These results are in accordance that an increase of  $S_i$  should be accompanied by a decrease in  $\Delta W$  because faster nucleation results in simultaneous creation of crystallites that grow to form more uniform crystallite's size distribution.<sup>23,38,39</sup> The initial slope  $S_i$  is higher for the compatibilized compounds than the uncompatibilized PP/midsole and PP/outsole compounds implied a faster rate of nucleation, which produces more uniformity of spherulite size. It has been reported that the width at half-height indicates the heterogeneity of the spherulite size.<sup>14,23,38,39</sup> The lower value of  $\Delta W$  for the compatibilized PP compound in our case, therefore, implied narrower distribution of crystallite size. The observed increase in  $\Delta H_{PP}$  values of the PP/midsole, PP/outsole and compatibilized PP/scrap dust compounds also indicate that the

added components influence the crystallinity of the PP.

Addition of the rubber phase results in an irregular texture of spherulite and smaller spherulite diameter.<sup>15,36,37</sup> Optical micrographs (crossed polars) of unfilled and filled PP were also used to analyze the crystallization behavior of the PP. Figure 4 show that plain PP crystallized in a macrospherulitic superstructure and the PP phase in the presence of midsole and outsole also exhibited crystallized structure like a macrospherulitic superstructure. However, the macrospherulites of the compound appear in size to be smaller than those of the plain PP. Not only the spherulite size, but also the spherulite structure of the spherulite is changed, markedly by the incorporation of the scrap dust for both midsole and outsole. It was seen that addition of the scrap dust resulted in a less regular spherulite texture with less sharp spherulite boundaries. This is due to heterogeneous nucleation and an increase in number of nucleation sites when scrap dust was incorporated.<sup>36,37</sup>

For the compatibilized compound with SBS, SEBS, SEBS-g-MA, and PE-g-MA the structure is still macrospherulitic, with a slight decrease in the spherulite

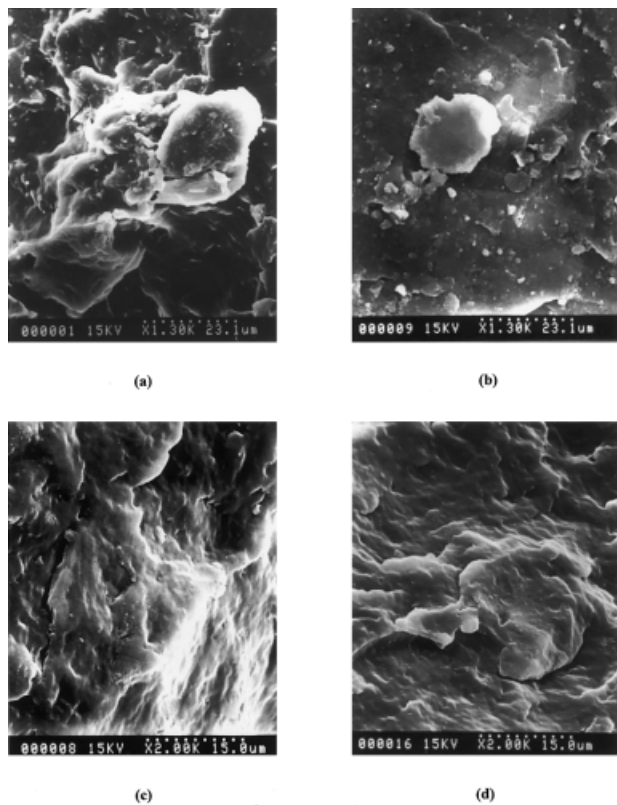


**Figure 6** SEM micrographs of cryofractured surface of uncompatibilized compound and compatibilized compound with 10 phr SEBS loading; (a) PP/midsole, (b) PP/outsole, (c) PP/midsole/10 phr SEBS, (d) PP/outsole/10 phr SEBS.

dimensions when the content of compatibilizer increased, whereas for PP-g-MA and PP-g-GMA the structure is microspherulitic, and the size of the spherulite dramatically decreased. Figure 5 clearly shows the decrease of spherulite size of PP in the PP/midsole and PP/outsole compounds compatibilized by PP-g-MA compared to the compound compatibilized by SEBS. Therefore, the perfection and size of the crystallite and degree of crystallinity in the compound play important roles on the properties of the PP compound.

**Morphology**

The interfacial tension between the two polymers is very important for phase morphology, and the added compatibilizer plays a major role in reducing interfacial tension and thereby forming a finer morphology.<sup>31-35</sup> In this study the SEBS and SEBS-g-MA copolymers are considered to be the best compatibilizers for the PP/scrap rubber dust compounds. The SEM micrographs of the cryofractured surface of uncompatibilized and compatibilized both PP/midsole and PP/outsole in Figure 6 show the typical morphology of an immiscible compound of the scrap rubber dust both midsole and outsole, which are larger size and larger

protrusions of the dispersed phase. After addition of the SEBS, the compatibilized compounds for both PP/midsole and PP/outsole show different features, smooth and polished surfaces, and more homogeneous in appearance than the distinct two phases.<sup>19</sup> The morphology suggested that the SEBS appears to span at the interfaces between regions of scrap rubber dust and PP, thus enhancing adhesion and compatibilization of the compound.<sup>30</sup>

Deformation mechanisms of the rubber-toughened polymers concern crazing, shear yielding and cavitation of the rubber particle.<sup>13</sup> Figure 7 shows the SEM micrographs of the fracture surface from impact testing of unfilled PP and PP/rubber dust compounds. The deformation mechanism of virgin PP was found to be brittle fracture. The uncompatibilized PP/midsole and PP/outsole show large domain sizes wherein it appears some voids occurred between the dispersed phase and matrix as well as at the smooth surface of the matrix. In Figure 8 the compounds that were compatibilized with 10 phr SEBS and SEBS-g-MA both in PP/midsole and PP/outsole showed the evidence of elastic formation occurred at the interface between the PP matrix and scrap dust particles to form fibrils (see arrow). The observation of fibril structure can be used to explain the improvement in toughness of the compound as reported previously. In addition, the occur-

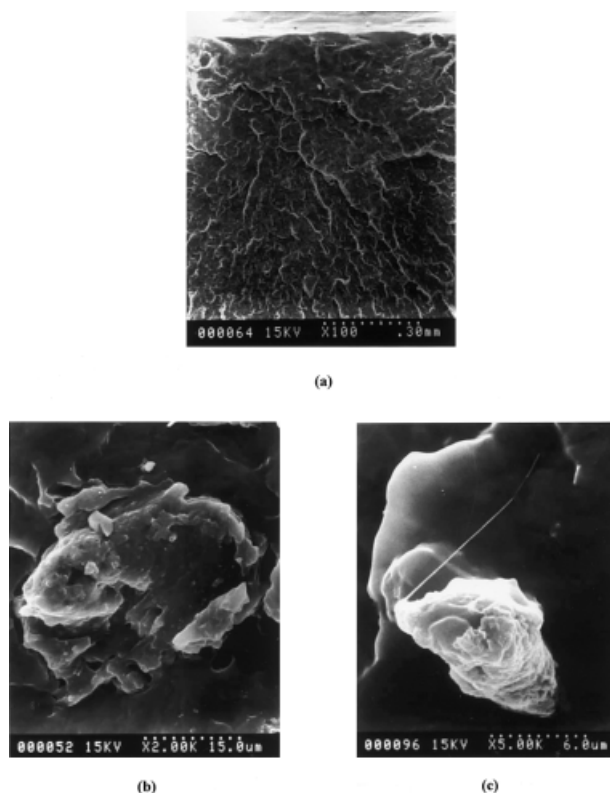


**Figure 7** SEM micrographs of impact fracture surfaces of unfilled PP and filled PP (a) neat PP, (b) PP/midsole, (c) PP/outsole.

rence of voiding and filaments at the interface between the PP and dispersed phase can be shown that the void formation may be due to cavitation localized at the rubber particle/matrix interfaces. Therefore, it can be concluded that increasing impact strength of the compatibilized compound with SEBS and SEBS-g-MA is due to formation of fibril texture between the phases. It can be expected that the improved impact values were achieved because of the good compatibility of components at the interface of polypropylene/scrap rubber dust compound. At the same time, the average dimensions of the dispersed phase decreases, and interfacial adhesion between the polypropylene and scrap rubber dust is also improved.

The fracture surface of the compatibilized PP/midsole compounds etched in xylene for 24 h were analyzed by SEM and shown in Figure 9. The morphology of unetched compatibilized compounds with SEBS and SEBS-g-MA are shown in Figure 9(a) and (b), whereas the etched compounds are in Figure 9(c) and (d). Holes were observed after etching the samples. In the case of the compatibilized compound with SEBS, small holes were found, and they were better dispersed than in the case of the compatibilized compound with SEBS-g-MA. The EB block in SEBS has normally a good compatibility with the PP.<sup>19</sup> The presence of polar succinic anhydride groups of the maleinated SEBS may cause stronger repulsion of the polar

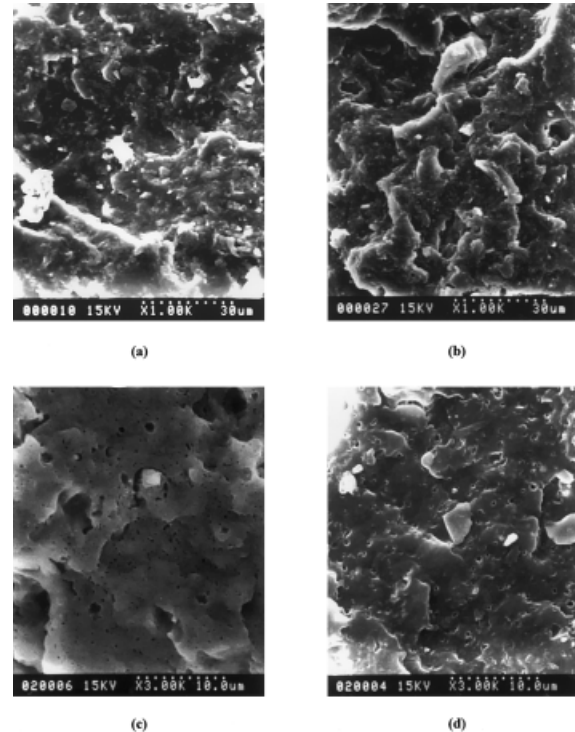


**Figure 9** SEM micrographs of unetched and etched samples of compatibilized PP/midsole (10 phr compatibilizers); (a) unetched PP/midsole/SEBS, (b) unetched PP/midsole/SEBS-g-MA, (c) etched PP/midsole/SEBS, (d) etched PP/midsole/SEBS-g-MA.

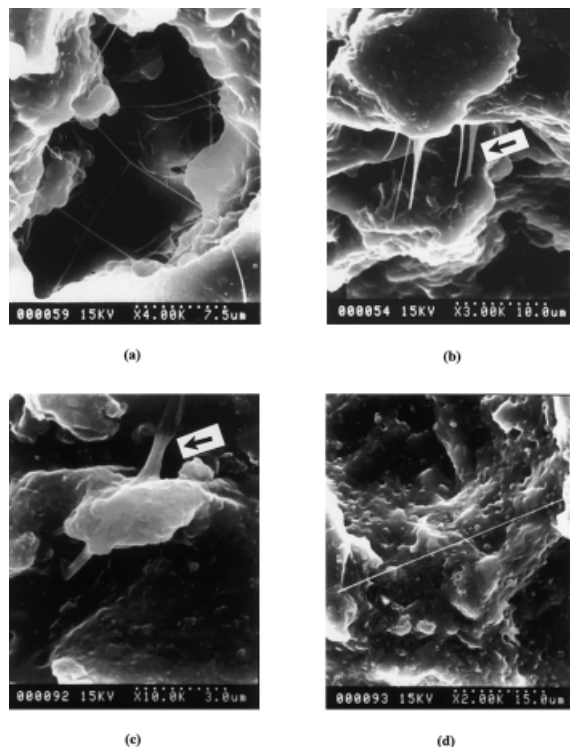


**Figure 8** SEM micrographs of impact fracture surfaces of compatibilized compound of PP/scrap dust (10 phr compatibilizer); (a) PP/midsole/SEBS, (b) PP/outsole/SEBS, (c) PP/midsole/SEBS-g-MA, (d) PP/outsole/SEBS-g-MA.

groups with the nonpolar PP. This corresponds to the impact value of the compound where addition of SEBS gave higher impact strength than when SEBS-g-MA was used. Therefore, it can be concluded that both SEBS and SEBS-g-MA can act as an impact modifier and compatibilizers in the compound.

## CONCLUSIONS

Development of impact strength of polypropylene/scrap rubber dust blend can be achieved by the addition of a compatibilizer. The good compatibilizer for the midsole and outsole dust were SEBS and SEBS-g-MA, which appear to function both as impact modifier and compatibilizer for PP/scrap rubber dust compounds. The SEBS and SEBS-g-MA content in the compound is expected to be a key variable affecting the toughness of PP/scrap dust compounds. The loading of the compatibilizer that gave the best impact properties to the PP compound was 10 phr. The SEBS was the best compatibilizer for PP/midsole compound; the impact strength was improved 90%, whereas in the PP/outsole compound the SEBS-g-MA was the best compatibilizer, and the impact strength was improved 86%.

By optical microscopy, it was found that the compound that gave good impact strength showed small



particle size and narrow distribution of the particle size. This is due to the fact that the good compatibilizer contributed to reducing the particle size of the scrap dust in the PP compound. This will reduce the interfacial tension between the phases, to prevent coalescence between minor phase particles and to improve the adhesion between the phases, which in turn, should contribute to an improved dispersion of the scrap rubber dust phase. The SEM micrographs of the compatibilized compounds with SEBS and SEBS-g-MA also showed the reduction of rubber dust into small rubber particle size in the compounds and the appearance of some fibril structures.

The tensile strength and the modulus of the compatibilized compound were slightly decreased, whereas the elongation at break was increased, which indicated the improvement of adhesion between phases. The value of elongation at break was dependent on the type of compatibilizer and compatibilizer loading. The best elongation at break was observed in PP/midsole compatibilized with SEBS, which was 450% improvement comparing to uncompatibilized compound.

This research was supported by the National Metal and Materials Technology Center. The authors would like to thank several companies for providing various polymers: Piyavat Rubber Industry Co. Ltd, Thailand, for the recycled rubber dusts; HMC Co. Ltd., Thailand, for polypropylene; Shell Chemical Co. Ltd. and Mitsui Co. Ltd. for some compatibilizers; Professor Gua Hua Hu, Laboratory of Chemical Engineering Sciences; Ecole Européenne D'Ingénieurs en Génie des Matériaux, CNRS-ENSIC-INPL France for PP-g-MA and PP-g-GMA.

## REFERENCES

- Murphy, J. *Plastics Additives & Compounding* 1999, 1, 18.
- Phadke, A. A.; De, S. K. *Polym Eng Sci* 1986, 26, 1079.
- Oliphant, K.; Baker, W. E. *Polym Eng Sci* 1993, 33, 166.
- Pramanik, P. K.; Baker, W. E. *Plast Rubb Comp Proc Appl* 1995, 24, 229.
- Haggstrom, B. *Proceeding in the Polymer Processing Society (PPS), Innovation in Polymer Processing, December 1-3, 1999, Bangkok, Thailand*, p. 190.
- Coppola, F.; Greco, R.; Martuscelli, E.; Kammer, H. W.; Kummerlowe, C. *Polymer* 1987, 28, 47.
- D'Orazio, L.; Mancarella, C.; Martuscelli, E.; Polato, F. *Polymer* 1991, 32, 1186.
- Jancar, J.; DiAnselmo, A.; DiBenedetto, A. T.; Kucera, J. *Polymer* 1993, 34, 1684.
- D'Orazio, L.; Mancarella, C.; Martuscelli, E.; Sticotti, G.; Massari, P. *Polymer* 1993, 34, 3671.
- D'Orazio, L.; Mancarella, C.; Martuscelli, E.; Sticotti, G.; Ghiselini, R. *J Appl Polym Sci* 1994, 53, 387.
- Mehrabzadeh, M.; Nia, K. H. *J Appl Polym Sci* 1999, 72, 1257.
- Karger-Kocsis, J.; Kallo, A.; Kuleznev, V. N. *Polymer* 1984, 25, 279.
- Jang, B. Z.; Uhlmann, D. R.; Vander Sande, J. B. *J Appl Polym Sci* 1985, 30, 2485.
- Choudhary, V.; Varma, H. S.; Varma, I. K. *Polymer* 1991, 32, 2534.
- Wenig, W.; Asresahegn, M. *Polym Eng Sci* 1993, 33, 877.
- Van der Wal, A.; Nijhof, R.; Gaymans, R. J. *Polymer* 1999, 40, 6031.
- Jiang, W.; Tjong, S. C.; Li, R. K. Y. *Polymer* 2000, 41, 3497.
- Gupta, A. K.; Purwar, S. N. *J Appl Polym Sci* 1984, 29, 1595.
- Setz, S.; Stricker, F.; Kressler, J.; Duschek, T.; Mulhaupt, R. *J Appl Polym Sci* 1996, 59, 1117.
- Veenstra, H.; Van Lent, B. J. J.; Van Dam, J.; De Boer, A. P. *Polymer* 1999, 40, 661.
- Gupta, A. K.; Ratnam, B. K.; Srinivasan, K. R. *J Appl Polym Sci* 1992, 46, 281.
- Gupta, A. K.; Ratnam, B. K.; Srinivasan, K. R. *J Appl Polym Sci* 1992, 46, 1303.
- Gupta, A. K.; Ratnam, B. K. *J Appl Polym Sci* 1991, 42, 297.
- Yoon, L. K.; Choi, C. H.; Kim, B. K. *J Appl Polym Sci* 1995, 56, 239.
- Phinyocheep, P.; Axtell, F. H.; Maiseumsook, T. *Elastomer*, 1999, 34, 212.
- Axtell, F. H.; Phinyocheep, P.; Chanthasartratsami, N. *Proceeding in the Polymer Processing Society (PPS), Innovation in Polymer Processing, December 1-3, 1999, Bangkok, Thailand*, p 193.
- Bucknall, C.B. *Toughened Plastics*, Applied Science Publishers Ltd.: London, 1977.
- Fayt, R.; Jerome, R.; Teyssie, Ph. *Polym Eng Sci* 1987, 27, 328.
- Moon, H.-S.; Ryoo, B.-K.; Park, J.-K. *J Polym Sci Part B Polym Phys* 1994, 32, 1427.
- Horak, Z.; Fort, V.; Hlavata, D.; Lednický, F.; Vecerka, F. *Polymer* 1996, 37, 65.
- Horiuchi, S.; Matchariyakul, N.; Yase, K.; Kitano, T.; Choi, H.K.; Lee, Y. M. *Polymer* 1996, 37, 3065.
- Tang, T.; Lei, Z.; B. Huang, B. *Polymer* 1996, 37, 3219.
- Plawky, U.; Schlabs, M.; Wenig, W. *J Appl Polym Sci* 1996, 59, 1891.
- Jannasch, P.; Wesslen, B. *J Appl Polym Sci* 1995, 58, 753.
- Gonzalez-Montiel, A.; Keskkula H.; Paul, D. R. *Polymer* 1995, 36, 4621.
- Martuscelli, E.; Silvestre, C.; Bianchi, L. *Polymer* 1983, 24, 1458.
- Jang, B. Z.; Uhlmann, D. R.; Vander Sande, J. B. *J Appl Polym Sci* 1984, 29, 4377.
- Gupta, A. K.; Rana, S. K.; Deopura, B. L. *J Appl Polym Sci* 1992, 44, 719.
- Jafari, S. H.; Gupta, A. K. *J Appl Polym Sci* 1999, 71, 1153.